DESIGNING TOUGHER MICROSTRUCTURES BY 3D PRINTING OF CONTINUOUS FIBRE-REINFORCED COMPOSITES

Yentl Swolfs[1,2], Silvestre T. Pinho[1]

[1]Department of Materials Engineering, KU Leuven, Kasteelpark Arenberg 44, 3001 Leuven, Belgium
Email: Yentl.Swolfs@kuleuven.be
[2]Department of Aeronautics, Imperial College London, South Kensington Campus, SW7 2AZ, London, United Kingdom
Email: Silvestre.Pinho@imperial.ac.uk

Keywords: microstructural design, 3D printing, translaminar fracture toughness, continuous fibres

Abstract
The translaminar fracture toughness of composites is a crucial parameter for the damage tolerance of composite parts and the microstructure is known to affect this parameter. A finite element model was therefore developed that is capable of predicting the translaminar fracture toughness of a complex microstructure. This model revealed that interfaces between carbon and glass fibre composites can increase the translaminar fracture toughness. Compact tension tests on 3D printed samples confirmed this conclusion experimentally. These results open up new avenues for designing composite parts with improved damage tolerance by fibre-hybridisation.

1. Introduction

3D printing has revolutionised the field of polymers and metals by allowing the design of structures that are impossible to achieve using traditional manufacturing processes [1]. The field of fibre-reinforced composites has lagged behind in this respect, as all previous efforts focused on discontinuous fibres. This has changed recently, as printers capable of printing continuous carbon, glass and Kevlar fibre-reinforced composites are now available commercially. By allowing more design freedom, 3D printing allows the design of composite microstructures that were previously very difficult if not impossible to obtain. With bundle sizes down to 0.1 mm by 1 mm being possible, unique microstructures that lead to unique properties can be designed. Here, the focus is on the design of microstructures with improved translaminar fracture toughness by a combined numerical-experimental approach.

Several mechanisms can be exploited to maximise the translaminar fracture toughness by careful design of the microstructure. The microstructure of nacre offers an excellent example [2]. Its compliant layers between stiff fibre-reinforced layers help nacre to achieve a high fracture toughness. An equivalent approach in fibre-reinforced composites can be achieved by the use of interleaved films. Unfortunately, conventional manufacturing processes are typically limited to scenario (a) in Figure 1. For translaminar cracks, this interleaving mechanism becomes relevant only in scenario (b), but such microstructures are very difficult to achieve using conventional manufacturing processes. With 3D printing, both scenarios can be manufactured.

Excerpt from ISBN 978-3-00-053387-7

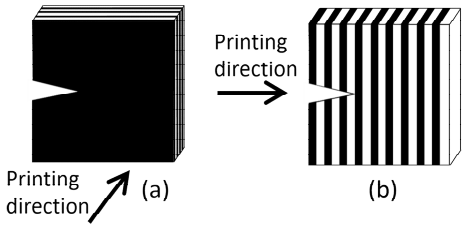

Figure 1: Potential microstructures that can be 3D printed and the direction in which they can be tested.

A finite element (FE) model of the compact tension test is developed that allows the incorporation of complex microstructures as well as size-dependent toughness of the constituents. This model is then used to predict microstructures that can lead to increased translaminar fracture toughness values. These microstructures are 3D printed and their translaminar fracture toughness is measured. In this initial study, the aim was to exploit potential synergies in hybrid composites consisting of carbon and glass fibre [3].

2. Finite element model

2.1. Model description

Since modelling an entire compact tension specimen as a solid part is both computationally expensive and unnecessary, only the fracturing region was modelled using 3D solid elements. The rest of the model uses 3D shell elements (see Figure 2). This drastically reduces the computational time but does not affect the accuracy of the predictions. The model has a width, height and thickness of 65, 60 and 1.8 mm respectively. The solid region has a total height of 6 mm and a length of 32 mm. The load is applied at 14 mm from the left-hand side and 16 mm from the symmetry plane. The initial crack length relative this location is 25 mm. A displacement of 2 mm is applied to both loading points with a smooth amplitude, resulting in a maximum relative displacement of 4 mm achieved over a time of 50 seconds.

The shell regions consist of quadrilateral shell elements with reduced integration. The solid region consist of hexahedral elements with a mixture of reduced and full integration. Full integration elements are used for elements that were 0.2 mm or less away from the cracking region. This helps to avoid element distortion and hourglassing, while the use of reduced integration elements elsewhere improves the computational efficiency.

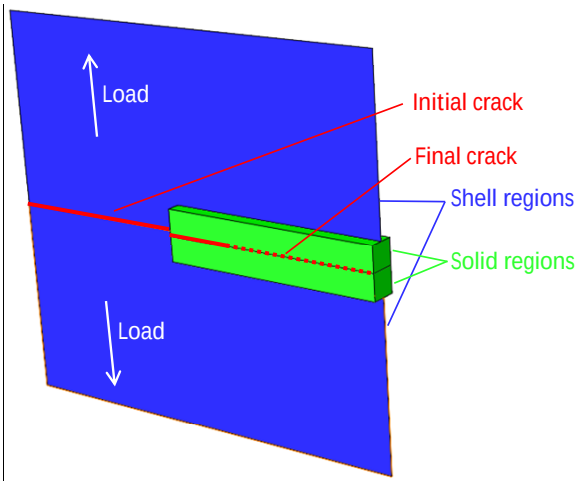

Figure 2: Visual representation of the FE model consisting of solid and shell regions.

Excerpt from ISBN 978-3-00-053387-7

The material parameters correspond to either a carbon or to a glass fibre-reinforced composite. A balanced 0/90 layup is assumed for calculating the engineering constants of the laminate (see **Table 1**). The cracking region is represented by a bilinear cohesive law with an initiation strength σ_{init} (see **Table 1**). At the interface between carbon and glass fibre regions, some nodes would be subject to the cohesive law for both the carbon and glass fibre composite. To avoid this problem, the interface between both materials is separated by cohesive elements. These cohesive elements are given a very high strength and are made very thin, and therefore did not affect the outcome of the model.

Table 1: Engineering constants and translaminar fracture toughness of the two reference composites.

	E_1 (GPa)	E_2 (GPa)	E_3 (GPa)	υ_{12} (GPa)	υ_{13} (GPa)	υ_{23} (GPa)	G_{12} (GPa)	G_{13} (GPa)	G_{23} (GPa)	G_{Ic} (kJ/m²)	σ_{init} (MPa)
Carbon fibre composite	62.0	62.0	6.9	0.036	0.036	0.036	3.6	3.6	3.6	50	1000
Glass fibre composite	23.1	23.1	9.3	0.13	0.13	0.13	3.4	3.4	3.4	100	500

The simulations were performed in Abaqus Explicit with a time step of 50s and a mass scaling factor of 10^4. This ensured that the kinetic energy was less than 2% of the strain energy. The linear and quadratic bulk viscosity were set to 0.02 and 0.4 respectively. The viscous dissipation, distortion control and artificial energies were always less than 5% of the strain energy. Nevertheless, oscillations in the force values were inevitable. These were hence averaged over a range equivalent to about 0.15s, which removed the majority of the oscillations. The fracture toughness at a given time increment was calculated by extracting the traction and crack opening displacement and integrating the resulting cohesive law.

Three different models were created (see **Figure 3**). These are labelled according to the progression that cracks sees as it grows, with CF and GF indicating the carbon and glass fibre composites, respectively.

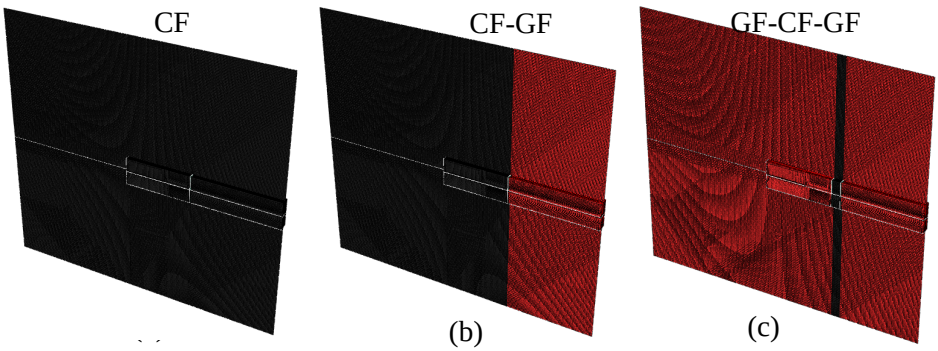

Figure 3: Illustration of the different models: (a) CF, (b) CF-GF, (c) GF-CF-GF.

2.2. Results

The force-displacement diagrams (see Figure 4a) reveal that the oscillations have not been filtered out completely. This also results in the variations in the toughness values in Figure 4b. The encouraging result however is that the GF-CF-GF model reached fracture toughness values higher than both reference composites. This 8.5% increase relative to the fracture toughness of the glass fibre composite is particularly impressive given that this was achieved by inserting CF, which is more brittle than GF. Additionally, the model crashed at this point due to the high resistance against crack propagation. The actual increase is therefore likely to be even higher.

Excerpt from ISBN 978-3-00-053387-7

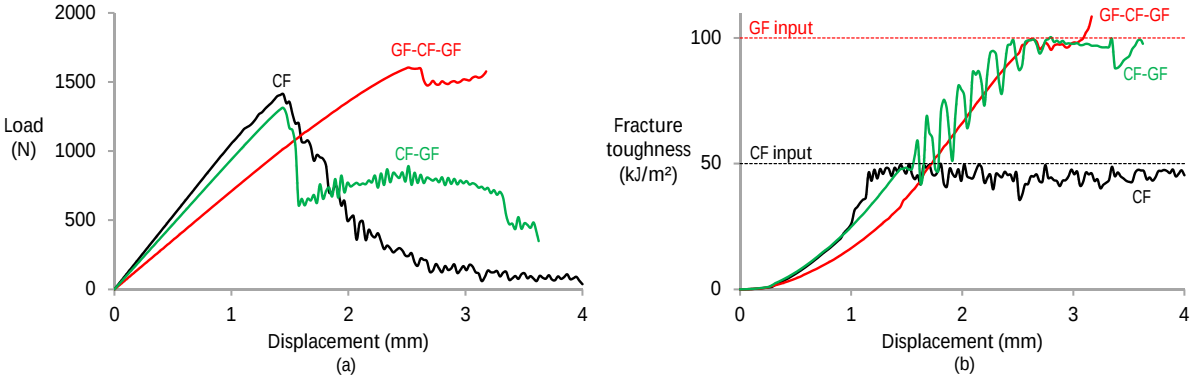

Figure 4: Modelling results: (a) load-displacement diagrams and (b) the evolution of the fracture toughness with time.

3. Experimental validation

3.1. Materials and production

Standard nylon, carbon fibre/nylon and glass fibre/nylon spools from MarkForged were used on a MarkOne printer. The nylon matrix is a blend of different grades with a measured tensile modulus of 0.45 GPa. The fibre volume fraction was measured to be 31% and each ply was 100 µm thick. A 5 mm thick sample with only 0° fibres was printed first. About 3.8 mm of this thickness consisted of glass fibres, whereas the outer nylon walls contributed about 1.2 mm. Eight layers of 90° fibres were the printed on either side of this sample to prevent splitting along the loading holes.

Four samples were successfully manufactured and tested. Three of the samples consisted of only glass fibre/nylon. The fourth sample was a hybrid, as the central 0° ply had a strip of 10 carbon fibre plies of 100 µm each.

3.2. Test methodology

The combination of high toughness and limited bonding between the layers made testing the samples challenging. To help limit the compressive forces, the double-tapered sample design from Blanco et al. [4] was used. The overall shape, the loading holes and a part of the notch were waterjet cutted. The notch was later machined to its final dimensions using a circular saw. An edge groove, as in the ASTM E1820 standard, was machined in by a 50 mm diameter blade with a thickness of 800 µm. This groove stopped at 5 mm from the edge of the sample to ensure sufficient material was left to withstand compressive failure. The depth of the groove on both sides was set to leave about 1 mm of the 0° ply intact. The exact thickness of the groove could not be determined beforehand, but was measured using scanning electron microscopy of the fracture surface.

Two anti-buckling guides were added to the top and bottom of the samples. Each guide is essentially a steel plate that prevents buckling of the specimens. Both halves of each guide are clamped together by two M8 bolts that are tightened by hand. This still allows relative sliding of the sample, and therefore does not affect the measurements.

Digital image correlation was used to track the distance at the notch on the line between the two loading holes. Data reduction was done by the compliance calibration method [5]. The plasticity of the nylon matrix however hampered a reliable fit with the experimental data. The obtained compliance calibration was therefore fitted to the experimental diagram of compliance versus crack length. In averaging the R-curves to obtain the average fracture toughness, the initial increase was not taken into account. The last part of the diagram was also not taken into account, as this part was affected by the edge groove being less deep.

Excerpt from ISBN 978-3-00-053387-7

3.3. Results

The R-curves for the four tested samples are shown in **Figure 5**. The average fracture toughness for the full glass fibre samples was 386 + 179 kJ/m², compared to 500 kJ/m² for the hybrid sample. This difference is not statistically significant due to the large standard deviation for the full glass fibre samples. The remarkable result is however that the carbon fibre strip has caused an increase in the R-curve.

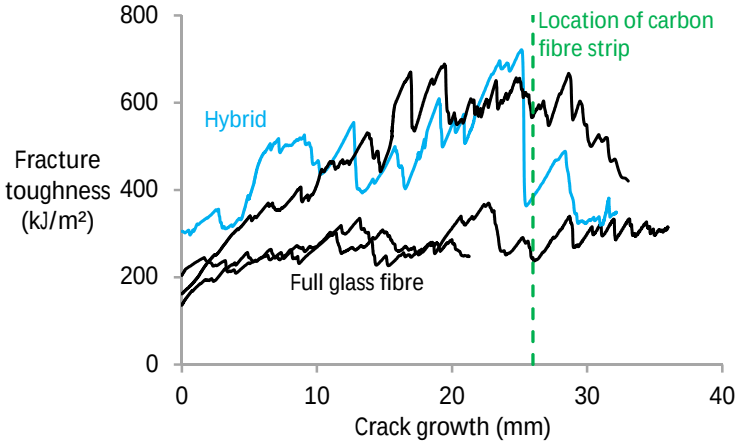

Figure 5: R-curves for the four tested samples, with the green dashed line indicating the locating

4. Conclusions

The results revealed that hybrid composites can be used to achieve translaminar fracture toughness values that are higher than the toughness of the constituents. A model has been developed that is capable of optimising the microstructure, and a manufacturing and testing methodology was devised that can be used to validate the model. In the future, the model will be used to further optimise the microstructure and reveal the optimised microstructure. This optimised microstructure and others will then be tested experimentally.

Acknowledgments

The authors acknowledge the support of the European Commission for the Marie Sklodowska-Curie Individual European Fellowship “HierTough” for YS. YS acknowledges the support of FWO Flanders for his postdoctoral fellowship. STP acknowledges EPSRC for his “NextGen” fellowship.

References

[1] L.J. Love, V. Kunc, O. Rios, C.E. Duty, A.M. Elliott, B.K. Post, et al. The importance of carbon fiber to polymer additive manufacturing. *J Mater Res*. 29:1893-1898, 2014.
[2] O. Kolednik, J. Predan, F.D. Fischer, P. Fratzl. Bioinspired Design Criteria for Damage-Resistant Materials with Periodically Varying Microstructure. *Advanced Functional Materials*. 21:3634-3641, 2011.
[3] Y. Swolfs, L. Gorbatikh, I. Verpoest. Fibre hybridisation in polymer composites: a review. *Composites Part A: Applied Science and Manufacturing*. 67:181-200, 2014.
[4] N. Blanco, D. Trias, S.T. Pinho, P. Robinson. Intralaminar fracture toughness characterisation of woven composite laminates. Part I: Design and analysis of a compact tension (CT) specimen. *Engineering Fracture Mechanics*. 131:349-360, 2014.
[5] S.T. Pinho, P. Robinson, L. Iannucci. Fracture toughness of the tensile and compressive fibre failure modes in laminated composites. *Composites Science and Technology*. 66:2069-2079, 2006.

Excerpt from ISBN 978-3-00-053387-7